

Physical Properties of Spicules from Simultaneous Spectro-Polarimetric Observations of He I and Ca II Lines

H. Socas-Navarro¹

D. Elmore¹

High Altitude Observatory, NCAR², 3450 Mitchell Lane, Boulder, CO 80307-3000, USA

navarro@ucar.edu

ABSTRACT

We present full Stokes observations from SPINOR in the Ca II infrared triplet and the He I multiplet at 1083 nm from which some properties of spicules have been derived. There are important advantages in multi-line observations, particularly from different elements. We find that the orientation of the plane of polarization is very different for the Ca and He lines, which provides the first direct model-independent evidence for magnetic fields in spicules. Our data shows that the Ca and He lines have almost identical widths. Since the Ca atom is 10 times heavier than He, we are able to conclude that most of the broadening is non-thermal ($\simeq 16 \text{ km s}^{-1}$) and to set an upper limit of 13 kK to the spicular temperatures. The bisectors of the lines span a velocity range of over 15 km s^{-1} for the He line and 30 km s^{-1} for the Ca ones. The vertical gradient of line-of-sight velocities is also very different for both elements. We obtain $2.8 \text{ km s}^{-1} \text{ Mm}^{-1}$ from He versus $6.4 \text{ km s}^{-1} \text{ Mm}^{-1}$ from Ca. These properties, and others from similar observations, should be taken into account in future physical models of spicules.

Subject headings: line: profiles – Sun: atmospheric motions – Sun: magnetic fields – Sun: chromosphere – stars: atmospheres

¹Visiting Astronomer, National Solar Observatory, operated by the Association of Universities for Research in Astronomy, Inc. (AURA), under cooperative agreement with the National Science Foundation.

²The National Center for Atmospheric Research (NCAR) is sponsored by the National Science Foundation.

1. Introduction

Spicules are elongated, nearly-vertical structures visible in emission above the solar limb in chromospheric lines. First observed over 100 years ago (Secchi 1887), spicules have thus far eluded our efforts to understand their physical nature and origin. Once viewed as a very attractive problem for solar physicists, interest seemed to fade away somewhat since the early 1970s. Most of the knowledge gathered until then, mainly from spectroscopic observations of H α , He D₃ or Ca H and K, is compiled in a comprehensive review by Beckers (1968). Since then, very few works have been published with new observational properties of spicules and some authors have concentrated instead in novel modeling efforts (the most recent by De Pontieu et al. 2004).

However, this scenario seems to be about to change drastically. Modern spectro-polarimeters capable of observing chromospheric lines off of the solar limb are providing new observational constrains that show considerable promise to expand our knowledge on spicules (and other chromospheric structures). In addition to the present work, there are two other papers in press with new spectro-polarimetric observations of He I lines, namely the 1083 nm multiplet (Trujillo Bueno et al. 2004) and D₃ (López Ariste & Casini 2004). Hopefully, this surge is only the beginning of a renewed interest in spicule observations. New data is needed both to inspire and to constrain future theoretical models.

We present here for the first time observations of spicules in the Ca II infrared triplet (in particular the 849.8 and 854.2 nm lines), alongside the He I multiplet at 1083 nm. The dataset analyzed here was recorded using the new SPINOR (Spectro-Polarimeter for INfrared and Optical Regions) instrument, at the Dunn Solar Telescope (DST) in the Sacramento Peak Observatory. We believe that multi-line observations from different elements (ideally with very different atomic weights) have important advantages to determine some magnetic, thermal and dynamic parameters of spicules. For example, we present evidence of the existence of a magnetic field in spicules without having to resort on complex Hanle effect modeling. In this sense, our work can be considered the first model-independent verification of the magnetic nature of spicules (although such fields have been obtained from Hanle effect measurements by Trujillo Bueno et al. 2004; López Ariste & Casini 2004). Since the thermal broadening depends strongly on the atomic weight, multi-line observations are also helpful to set boundaries to this type of broadening.

2. Observations

The observations that we report on were obtained on 19 June 2004 with the following SPINOR configuration. We used a spectrograph grating with 308 lines/mm. The ASP cameras (256 by 256 pixels) were set to record the Ca II lines at 849.8 and 854.2 nm. The new SPINOR Pluto camera (488 by 652 pixels) was set to the He I multiplet at 1083 nm.

The spectrograph slit had a width of $80\text{ }\mu\text{m}$, which corresponds to an angular size of $0.6''$ on the DST focal plane. Short scans of 10 steps were observed at various positions on the solar limb. The scanning step was chosen to be $0.22''$, which is significantly smaller than the typical angular resolution ($\sim 1''$). This was done so that it would be possible to bin multiple images in the scanning direction, thus increasing the signal to noise ratio without saturating any of the detectors. This approach is useful for multi-line observations, particularly when significant variations exist among the quantum efficiencies of the cameras or the photon flux they receive. In this case, the ASP cameras are observing a spectral region where they have a quantum efficiency of $\sim 30\%$, whereas the Pluto camera has only $\sim 3\%$ efficiency near $1\text{ }\mu\text{m}$.

The polarization modulator used in this run was not the new SPINOR achromatic bycristaline modulator, which we had not yet received from the vendor at the time of these observations³. We were able to use the ASP modulator which, although not optimal, still provides some modulation at these wavelengths. The linear polarization efficiency obtained with our setup was $\simeq 26\%$ at the wavelength of the Ca lines and $\simeq 15\%$ at the wavelength of the He multiplet. For circular polarization we obtained 36% and 17%, respectively.

The main limitation of our observations is probably the low signal level in the 1083 nm region, due to the combination of low detector and polarimeter efficiency discussed above. Nevertheless, there is still sufficient signal especially in the bright emission cores of the lines to allow for a detailed study of some important spicule properties.

An occulting disk at the telescope prime focus was inserted to block the bright photospheric emission. This is helpful to reduce the amount of stray light from the solar disk which would otherwise contaminate the relatively faint spicule emission. The downside of this technique is that it complicates the data reduction and calibration by removing some references, such as quiet Sun intensity or telluric lines (useful for absolute wavelength determination). The polarization calibration also becomes more difficult because we no longer have continuum radiation to use as a source of unpolarized light.

The telescope was calibrated as explained in Socas-Navarro et al. (2004), using an

³The new polarization modulator is now available to users of the DST upon request.

array of achromatic polarizers on top of the entrance window. Calibration data were obtained simultaneously for the entire wavelength spectrum by means of a cross-dispersor in the beam before the detector. The datasets thus obtained were fitted with a wavelength-dependent model of the DST, allowing us to determine the optical parameters that characterize the telescope polarimetric response. Another set of achromatic polarization optics at the DST exit port was used to determine the Mueller matrix of the instrument.

Even after the exhaustive calibration outlined above, some residual cross-talk still remains from Stokes I into Q , U and V . In practice, this residual is usually determined from the continuum polarization (preferably at disk center, especially when observing at blue wavelengths where scattering polarization may be important). This was not possible in our observations because we only had spicule line emission (the photospheric continuum was blocked by the occulting disk). Fortunately, we also had disk observations of active regions from the same day. The spicule data reported here were taken only minutes away from an earlier sunspot observation. We used the residual cross-talk measured in the disk data to correct the spicule dataset.

Fig 1 shows the (polarized) spectra of a spicule at the three spectral regions, observed on the East limb of the Sun at -70° latitude. Notice the absence of signal in the Stokes V images (bottom row), which indicates that no residual cross-talk remains above the noise level. The real Stokes V signal one would expect to have is too weak to show in these images (Trujillo Bueno et al. 2004).

3. Results

Our observations show a bright emission core concentrated in the lower part of the image. Above this bright emission there is a diffuse faint tail that extends upwards and exhibits a strong redshift that increases with height. The brightest emission is seen in the core of 854.2. Interestingly, while 1083 has the weakest emission near the limb, the bright core extends higher than either one of the Ca lines (up to $\simeq 5''$ in He, as opposed to $\simeq 2''$ in Ca). The emission in 849.8 is weaker than in 854.2 and fades away very rapidly with height. The faint redshifted tail is not detectable in this line with our noise level.

Most of the discussion in this paper refers to the bright area near the limb (the lower $\simeq 2''$ in 849.8 and 854.2, and $\simeq 5''$ in 1083), as this is the region where we have stronger signals.

Let us start considering the Doppler widths of the lines. Fig 2 shows the result of fitting Gaussian curves to two of the spectral lines observed. The Ca atom is 10 times heavier than

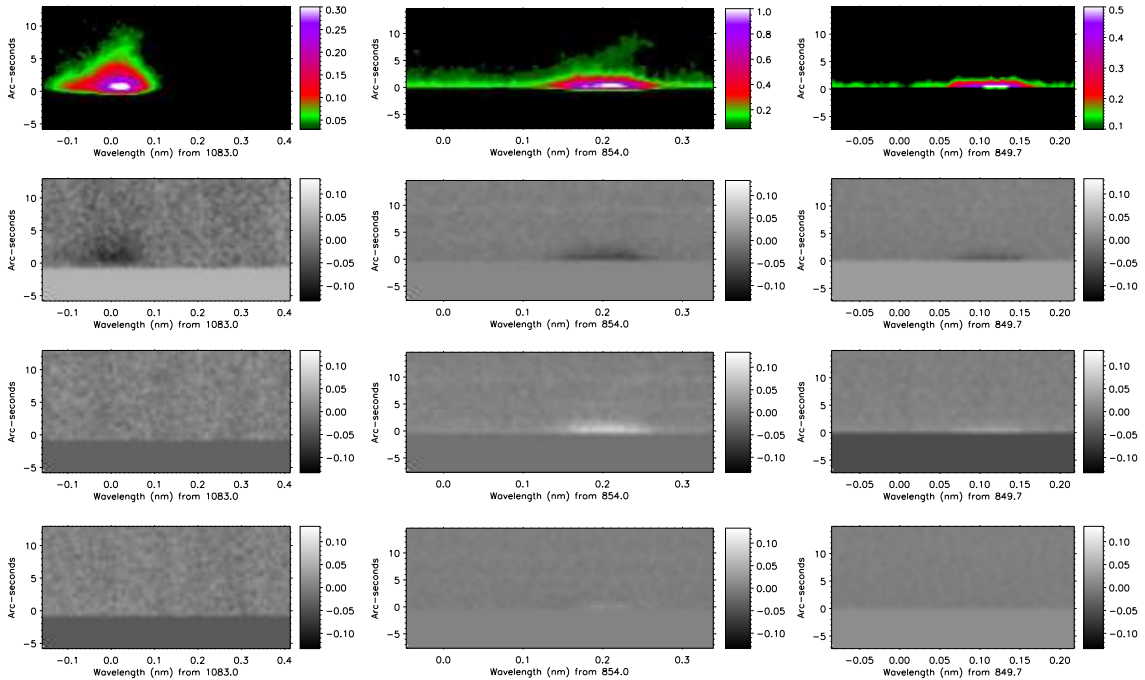


Fig. 1.— Stokes spectra of a spicule observed in the He I multiplet (left), and the Ca II lines at 854.2 nm (middle) and 849.8 (right). The Stokes parameters displayed, from top to bottom, are I , Q , U and V , respectively. The vertical scale is arc-seconds measured from the edge of the occulting disk. All profiles are normalized to the maximum intensity of the 854.2 nm line.

He. If the lines are broadened by microscopic thermal velocities, one would expect the He line to be over 3 times broader than those of Ca. However, this is not the case as all three lines have very similar widths. This indicates that the thermal broadening accounts only for a small part of the total line width. This conclusion is still valid even if the lines have some amount of optical thickness (which we shall neglect in this work), since this has a relatively little impact on the Doppler width (Trujillo Bueno et al. 2004), insufficient to explain the factor 3 discrepancy.

If we assume that the non-thermal broadening mechanism (rotation, expansion, etc) has the same effect on the three lines at a given spatial position, it is possible to establish an upper limit to the electron temperature of the spicule. Let us separate the total width as:

$$\Delta\lambda^2 = \Delta\lambda_T^2 + \Delta\lambda_N^2, \quad (1)$$

where $\Delta\lambda_T$ and $\Delta\lambda_N$ denote the thermal and non-thermal broadening, respectively. As we increase the temperature, $\Delta\lambda_T$ increases more rapidly for the He lines than for the Ca ones:

$$\Delta\lambda_T^{He} = \sqrt{10}\Delta\lambda_T^{Ca}, \quad (2)$$

which implies that the $\Delta\lambda_N$ also decreases more rapidly for He. If we assume a typical uncertainty of 1.5 km s^{-1} in $\Delta\lambda$ (taken from the difference between the fits to the two Ca lines), we can conclude that $T < 13 \text{ kK}$. For higher temperatures, $\Delta\lambda_N$ would be considerably smaller in the He lines than in those of Ca, which contradicts our initial assumption that $\Delta\lambda_N^{Ca} = \Delta\lambda_N^{He}$. A summary of these calculations is shown in Table 1.

Unfortunately, it is not possible to use a similar argument to obtain a lower limit. The reason is that, once $\Delta\lambda_T$ becomes small enough, the total broadening is dominated by the non-thermal component. In this regime, all three lines end up having the same width and are compatible with the observations regardless of the temperature.

It is also interesting to consider the far wings of the lines. Trujillo Bueno et al. (2004) noticed that their He observations had very extended wings when compared to those of a Gaussian. Our observations confirm their results for the He line (see Fig 2, right panel). However, we find that the Ca lines show the opposite behavior. Both Ca lines have wings that are actually *narrower* than those of a Gaussian (849.8 is shown in Fig 2, left). These results indicate that the far wings are probably dominated by the non-thermal broadening. It is not clear to us why the Ca and He wings would exhibit such a different behavior.

The observed profiles shown in Fig 2 (as well as that of the 854.2 nm line, not shown in the figure) exhibit signatures of differential Doppler shifts from the wings to the core of the lines. To study this in some more detail we calculated the bisector of all three lines (shown in Fig 3). For the 1083 nm line we have left out the lower part of the curve, to avoid

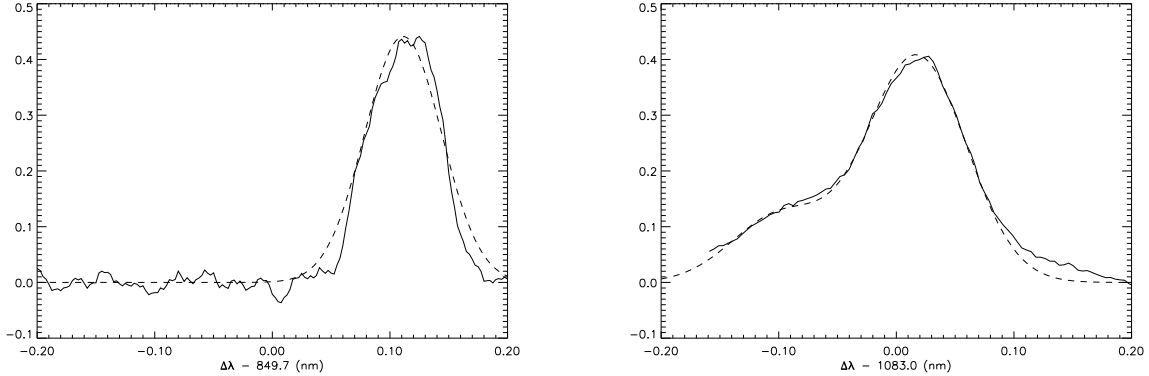


Fig. 2.— Gaussian fits to the observed Ca II line at 849.8 nm (left) and the He I multiplet at 1083 nm (right). The He I profile is fitted with two Gaussians of the same width centered at 1082.91 and 1083.03 nm, respectively. The fitted widths are: 18 km s⁻¹ for 854.2 (not shown), and 16.6 km s⁻¹ for both 849.8 and 1083. Both observed and synthetic profiles are normalized to the maximum intensity of the 854.2 nm line. The fits overestimate the wings of the Ca lines, but underestimate those of the He lines. Notice the relative Doppler shifts from the wings to the core of the Ca line.

Table 1.

	He I 1083 nm	Ca II 854.2 nm	Ca II 849.8 nm
Δλ (km s ⁻¹)	16.6	18.0	16.6
Δλ _N (km s ⁻¹), T = 10 kK	15.3	17.9	16.5
Δλ _N (km s ⁻¹), T = 13 kK	14.9	17.9	16.5
Δλ _N (km s ⁻¹), T = 15 kK	14.6	17.8	16.4
<dv/dh> (km s ⁻¹ Mm ⁻¹)	2.8	6.4	N.A.
U/Q ratio	0.07	-1.29	-0.88

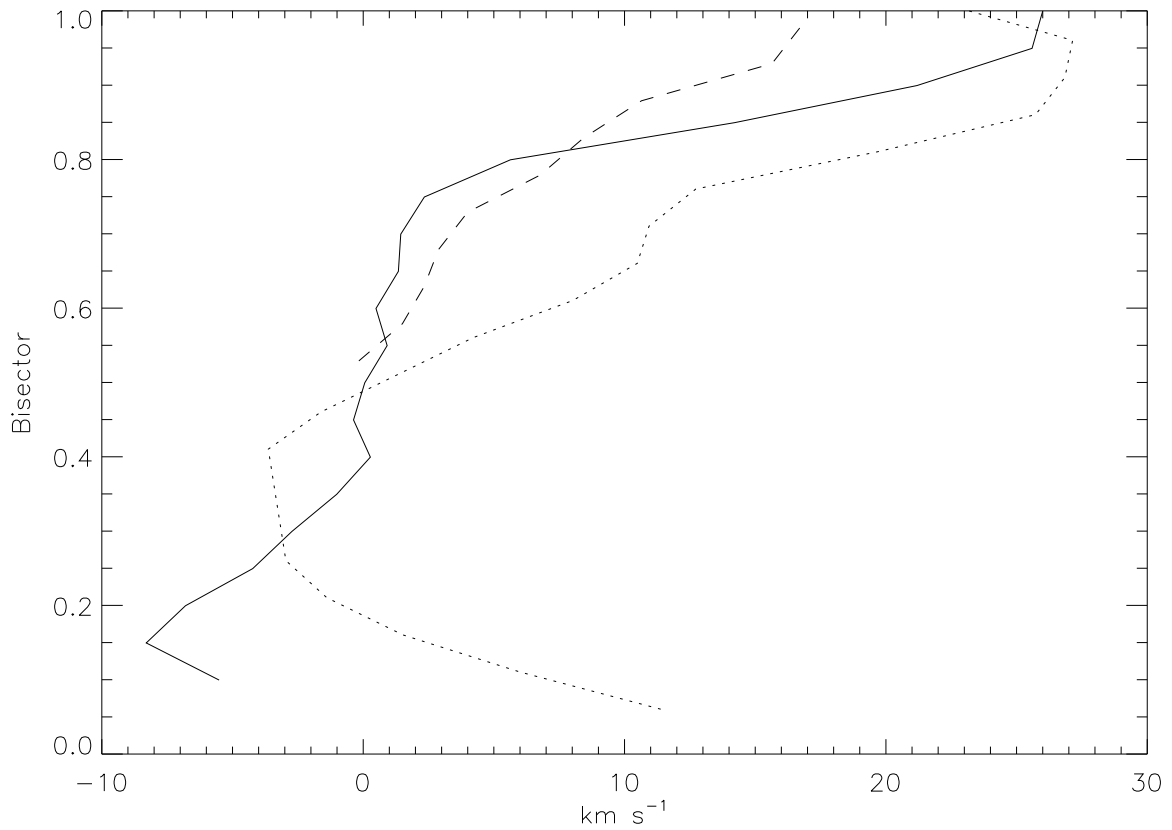


Fig. 3.— Bisectors of the lines at 854.2 (solid), 849.8 (dotted) and 1083 (dashed). Positive abscissa values correspond to redshifts. The zero point for all three lines is arbitrary due to the lack of a suitable absolute wavelength reference in the data.

the contamination introduced by the blend with the blue component of the multiplet. All three lines exhibit a strong redshift from approximately half of the profile to the core. This redshift is stronger in the Ca lines, where the relative velocities reach 30 km s^{-1} . The He line, on the other hand, reaches only some 17 km s^{-1} . The lower part of the 849.8 curve is also redshifted, producing a C-shaped bisector. This is not obvious in the 854.2 line, however. The interpretation of bisectors is not as straightforward as it is in disk observations, in which the vertical axis is directly related to height in the atmosphere. Here, a line profile may be viewed more as a histogram of velocities. The intensity at a given wavelength is related to the density of excited atoms with the corresponding Doppler shift. These curves might be helpful as a test for future physical models of spicules, in particular for the distribution of macroscopic velocities within the emitting plasma.

Fig 1 also shows that the faint tail visible at 854.2 and 1083 nm above the bright emission exhibit a height-dependent redshift. We have estimated the mean velocity gradient ($\langle dv/dh \rangle$) associated with the redshift in the range of heights between $5''$ and $7.5''$ (approximately between 3700 and 5500 km above the limb). The results are shown in Table 1 (fifth row). It is interesting to note that the mean gradient differs by more than a factor 2 between the Ca and He lines (recall that we are looking at the same spatial location along the slit). Only Krat & Krat (1961) have reported a similar disparity between spicule velocities as measured in different lines (in their case, between $\text{H}\alpha$ and He I D_3). This “interesting phenomenon”, as Beckers (1968) referred to it, would be very difficult to explain if one assumes that both emissions come from the same region. Instead, we propose that the line-of-sight integration is mixing together different structures in the observed pixel. The excitation conditions in these structures may be different, giving rise to stronger emission in either Ca or He and resulting in different apparent velocities for each line.

Let us now turn to the question of the possible presence of magnetic fields in spicules. It is not straightforward to measure such fields ($\sim 10\text{-}30 \text{ G}$, see Trujillo Bueno et al. 2004; López Ariste & Casini 2004) because the Zeeman splitting is too small to be detected in the broad intensity profiles of these lines, and the Stokes V signal is below the detection threshold (or very close to it). Even if such Zeeman signals could be detected, the lines would be formed in the so-called weak-field regime, in which it is not possible to separate the intrinsic field strength from its filling factor in the observed pixel.

The only possible diagnostics left for reliable magnetic field determinations is the Hanle effect. Still, the interpretation of Hanle observations is not trivial. One needs a precise knowledge of the zero-field polarization produced by the scattering of anisotropic radiation in the higher atmosphere. The Hanle effect then leads (typically) to some depolarization of the zero-field signal, as well as a rotation of the linear polarization plane. In some sense, one

essentially compares the theoretical zero-field polarization with the observations and ascribes the difference to the effect of a depolarizing magnetic field. It is therefore crucial to use a realistic model of the atmosphere and the illumination, especially in cases like the 1083 nm lines which are sensitive to coronal radiation.

To our best knowledge, the first claim that spicules are magnetized is the recent work by Trujillo Bueno et al. (2004) (but see also López Ariste & Casini 2004), who carried out a detailed Hanle modeling of the 1083 nm multiplet. Having multiple spectral lines in our observations allows us to confirm the presence of a magnetic field in spicules using a straightforward, model-independent reasoning. In the absence of a magnetic field, one would observe some degree of scattering polarization. The plane of polarization of this signal is given by the geometry of the scattering process and would be the same for all three lines observed here. If, on the other hand, the scattering atoms are embedded in a magnetic field, then the Hanle effect would rotate the plane of polarization by an amount that depends on some parameters of the transition. In this case, the orientation of the linear polarization would be different in different lines. It is clear from Fig 1 that the ratio of the Stokes Q and U signals is different for the Ca and He lines, implying a different orientation of the polarization plane (and therefore the presence of a magnetic field). The last row of Table 1 lists the values of U/Q averaged over the line core.

4. Conclusions

The observations that we present in this work provide some new insights into the physical origin of spicules. By observing lines of both Ca and He we are able to set constraints on the non-thermal broadening of the lines and the temperature of the emitting plasma. The change in the orientation of the polarization plane in the Ca and He lines is a convincing model-independent evidence for magnetic fields in prominences. A quantitative determination of the field strength and orientation would require detailed modeling of the line formation, which is beyond the scope of the present work. The different behavior of the emission wings in He and Ca (broader and narrower than a Gaussian, respectively) is certainly intriguing. It seems appealing to consider this as a clue for the nature of the non-thermal broadening mechanism.

In spite of recent efforts, spicules still remain poorly understood and we feel that more data are urgently needed. We plan to expand the results presented here in a forthcoming paper with new observations and more detailed analyses. In particular we intend to use an infrared camera and the new SPINOR modulator to obtain better signal-to-noise ratios in the infrared (which, as stated above is one of our main limitations here). Detailed Non-LTE

modeling would be desirable and it seems to be well understood now, at least for the Ca lines both in the Zeeman (Socas-Navarro et al. 2000) and Hanle (Manso Sainz & Trujillo Bueno 2001) regimes.

The authors are grateful to the Sac Peak observatory staff for their help with the observations, in particular D. Gilliam, M. Bradford and J. Elrod. Thanks are also due to R. Manso Sainz for suggesting a plausible explanation for the difference between Ca and He velocity gradients, and also for comments on an earlier draft of the manuscript.

REFERENCES

Beckers, J. M. 1968, *Solar Phys.*, 3, 367

De Pontieu, B., Erdélyi, R., & James, S. P. 2004, *Nature*, 430, 536

Krat, V. A., & Krat, T. V. 1961, *Izvestiya Glavnoj Astronomicheskoy Observatorii v Pulkove*, 22, 6

López Ariste, A., & Casini, R. 2004, *A&A, submitted*

Manso Sainz, R., & Trujillo Bueno, J. 2001, in *ASP Conf. Ser.* 236: Advanced Solar Polarimetry – Theory, Observation, and Instrumentation, 213

Secchi, A. 1887, "Le Soleil, Vol. 2" (Gauthier-Villars, Paris)

Socas-Navarro, H., Elmore, D., & Lites, B. 2004, *Solar Physics, submitted*

Socas-Navarro, H., Trujillo Bueno, J., & Ruiz Cobo, B. 2000, *ApJ*, 530, 977

Trujillo Bueno, J., Merenda, L., Centeno, R., Collados, M., & Landi Degl'Innocenti, E. 2004, *ApJL, submitted*